Experimental Study on Fluctuating Thermal Loads in Swept Shock Wave/Turbulent Boundary-Layer Interactions

Yeol Lee*

(*Received August 14, 1997*)

An experimental research program providing new knowledge of the fluctuating thermal loads in swept shock wave/turbulent boundary-layer interactions is described. An equilibrium turbulent boundary-layer on a flat plate is subjected to an impingement by the swept planar shock waves generated by a sharp fin. Two different fin angles at a freestream mach number of 4.0 produce relatively strong interactions. For each different interaction case the fluctuations of surface temperature in the interactions are obtained by miniature thin-film-resistance sensors connected to an anemometer. The distributions of properties of the surface temperature fluctuation, such as their rms levels and power spectra are obtained for each interaction. From the present measurement, the fluctuations of thermal loads near the reattachment of the separated flow under the λ-shock structure contains considerable high-frequency components, which is contrary to the previously observed unsteady phenomena of surface pressure in the same types of interactions.

Key Words: Thermal Loads, Surface Temperature Measurements, Fluctuation, RTD, Shock Wave, Boundary-Layer Interactions, Separation, λ-Shock.

Nomenclature

$G(f)$: Power spectral density
M_∞ : Freestream Mach number
M_n : Mach number normal to inviscid shock
α : Angle-of-attack of the fin
β : Angle with respect to incoming freestream direction, azimuth angle in spherical polar coordinates
δ : Boundary-layer thickness
δ^* : Boundary-layer displacement thickness
θ : Boundary-layer momentum thickness
φ : Elevation angle in spherical polar coordinates
σ_T : Rms (or standard deviation) of wall temperature fluctuations

1. Introduction

The study of shock wave/turbulent boundary-layer interactions is important for the solution of internal and external aerodynamic/aerothermal problems in the design of high-speed vehicles, as well as for the validation of the associated numerical simulations. Despite many previous studies of the overall problem, a little knowledge has been gained for the swept interactions until recently, and more extensive experimental work is still needed for a better understanding of the dynamics of such flows.

When an oblique shock wave of sufficient strength impinges upon a solid surface and interacts with the boundary-layer on that surface, a three-dimensional separated region is generated there. Peak values of surface pressure, skin friction and heat transfer are then observed to occur near the reattachment of this separated flow (Lu, 1988 ; Kim et al., 1991 ; Lee et al., 1994). These peak values are of great practical importance in establishing the limits of the aerodynamic and aerothermal loads on high-speed flight vehicles. Also, the turbulence structure and the unsteady shock motion result in fluctuations of pressure, skin friction, and heat transfer in such flows, which are sources of serious additional loads of

* Assistant Professor, Dept. of Aero. & Mech. Engr. The Hankuk Aviation University

an unsteady nature. Therefore, the knowledge of this unsteadiness in shock wave/bounday-layer interactions, which is the objective of the present experimental work, is critical in the design of high-speed vehicles.

Until to the present time, the characteristics of the unsteadiness have been revealed only by the empirical approaches. Furthermore, these unsteady phenomena in the shock/boundary-layer interactions have mainly been studied via fluctuating surface pressure measurements, using flush-mounted minature wall pressure transducers located underneath of the testing surface. The majority of such studies has been involved in two-dimensional interactions such as the interactions generated by the forward-facing steps and the compression corners (Kistler, 1964 ; Dolling and Murphy, 1983). Most studies have been concentrated on the dynamics of "separation". Characteristic feature observed in these two-dimensional interactions is the intermittent, low-frequency motion of the separation shock. Only recently, measurements in swept shock/boundary -layer interactions have been made (Gibson and Dolling, 1991 ; Erengil and Dolling, 1993). Garg and Settles (1966) also made detailed measurements of the unsteady surface pressure in Mach 3 and 4 sharp fin interactions. They found that the magnitude of these pressure fluctuations was largest near the primary attachment, dominated by relatively low-frequency fluctuations in the range of 0~5 kHz. Much of the information on unsteady phenomena in the shock/boundary-layer interactions has been reviewed by Dolling(1993).

The salient feature of the swept-sharp fin interaction is its quasi-conical symmetry. This has been observed by many investigators and recently confirmed by parametric studies (Lu and Settles, 1983 ; Alvi and Settles, 1991). Briefly, the interaction growth (not only the surface features, but also the flowfield structure above the surface) is conical with respect to virtual conical origin (VCO), except for an initial region in the immediate vicinity of the juncture of the fin-leading-edge and the flat plate (Zubin and Ostapenko, 1979). This quasi-conical symmetry in swept shock wave/boundary-layer interactions is even observed in the unsteady nature of the interactions. Gibson and Dolling (1991) measured wall pressure fluctuations in Mach 5 sharp-fin induced interactions, and found that the unsteadiness had conical characteristics in general. Reviews by Settles and Dolling (1986, 1990) cover the detailed progress of research on the swept interaction problem.

Since most of the previous studies on these unsteady phenomena in the interactions have been concentrated on the surface pressure measurements, the present experiments have been designed to assess the unsteady thermal load generated by such sharp-fin-generated swept interactions and to obtain a better understanding of such mechanism by comparing the present results with other previous data. Since the phenomenon of temperature fluctuations is believed to be close to the characteristics of heat transfer fluctuations, the present work will also bring a clue on the phenomena of heat transfer in the same type of interactions.

2. Experimental Methods

2.1 Wind tunnel facility and test conditions

The present experiments are performed in the Penn State University Gas Dynamics Laboratory' s supersonic wind tunnel facility, which is an intermittent blowdown tunnel with a test section size of $15cm \times 17cm \times 60cm$. The facility has a unique variable Mach number capability over the range of Mach 1.5 to 4.0 by way of an asymmetric sliding-block nozzle. A $57m^3$, $2.0Mpa$ pressure reservoir provides testing times up to 2 minutes at stagnation pressure up to 1.5 Mpa and a near -ambient stagnation temperature. The experiments described in this paper were performed at the freestream Mach number of 4.0, and tabulated data on the typical freestream test conditions are listed in Table 1.

2.2 Fin and flat plate

The interaction is generated by an equilibrium, near-adiabatic flat plate boundary-layer interacting with the swept, planar oblique shock wave generated by an upright, sharp-leading-edge fin

Table 1 Typcial Freestream Test Conditions.

Total pressure	1.48 Mpa
Total temperature	288 K
Freestream velocity	662 m/sec
Freestream density	0.52 kg/m^3
Wall temperature	276 K
Mass flow rate	8.0 kg/sec

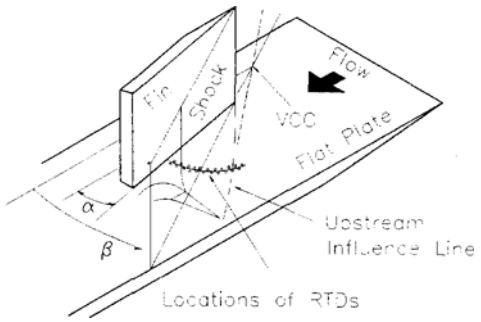

Fig. 1 Sketch of test geometry.

at an angle of attack, α (see Fig. 1).

The fin leading edge is 21.6 cm aft of the plate leading edge. The size of the fin is small enough to avoid blockage of the flow, but large enough to generate a "dimensionless semi-infinite" interaction (Settles and Dolling, 1986) on the flat plate. The strength of the interaction is controlled by changing the angle of attack of the fin, and the movement of the fin is manipulated by a pneumatic fin-injection mechanism, which is mounted through the tunnel side wall. The present flat plate is a sandwich consisting of a top sheet of 37 resistance temperature detectors (RTDs), a foil heater, an insulation board, and a stainless steel supporting plate. The foil heater can be used to generated uniform heat flux of the surface and elevate the surface temperature of the plate. Utilizing the temperature-calibration and the heat generation from the thin-foil heater underneath the RTDs, the present sandwiched plate can be used to measure the steady-state heat transfer in the interactions (Lee et al., 1994). However no heat is generated from the foil heater for the present test, and only surface temperature fluctuations in the interactions are measured by the RTDs connected to an anemometer.

2.3 RTD surfact temperature sensors

Custom-made thin-film temperature sensors (RTDs) are vacuum-deposited on a plastic substrate by NASA-Langley Research Center using microlithographic fabrication techniques. These thin-film sensors can measure accurate surface temperatures without disruption of the flowfield and have a characteristic of high frequency response (reported as order of microseconds). Each of the 37 RTDs consists of a Nickel-film resistance thermometer of about 1000 Angstroms thickness deposited on the 50 μm-thick Kapton polyimide substrate sheet. The sheet itself is then attached to the flat surface of the foil heater using laminating epoxy. Nickel is chosen as the sensing element because of its relatively high sensitivity and its excellent adhesion characteristics in thin-film applications. The individual sensor geometry is the square 1×1 mm serpentine pattern as shown in Fig. 2(a). This pattern maximize the sensor length in a small surface area, thus producing a high room-temperature resistance (65Ω), a high signal-to-noise ratio, and effectively a "point" surface temperature measurement. Low-resistance 6μm-thick copper-film leads are also deposited from each sensor to the edge of the polyimide sheet, and finally connected to an anemometer.

To utilize the conical nature of the fin interactions which is mentioned earlier, a double-circular-arc distribution of the 37 RTDs (at radii of 86 mm and 91 mm from the fin leading edge) is chosen as shown in Fig. 2(b). In terms of the angle measured with respect to fin leading-edge, these gages are spaced at a 2° angular separation from 6° to 78° for high data resolution.

2.4 Turbulent boundary-layer on flat plate

The undisturbed incoming boundary-layer on the flat plate without fin is two-dimensional and turbulent. Natural boundary-layer transition on the plate typically occurs within $1\sim2$ cm of the flat-plate leading edge at the present high Reynolds number flows. The flat plate has a

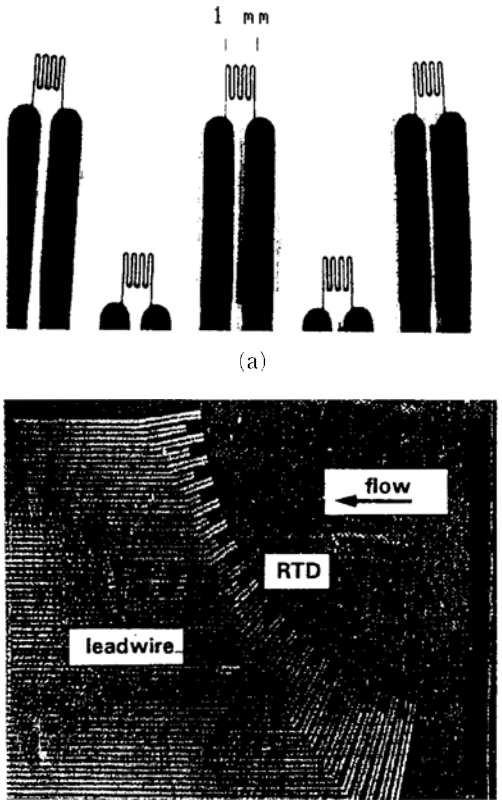

Fig. 2 Thin-film sensor (RTD) array : (a) individual sensor geometry, (b) radially-distributed RTDs on a flat plate.

negligible pressure gradient and the turbulent boundary-layer on the flat plate is naturally in a near-adiabatic condition (the ratio of the wall temperature, T_w, to the adiabatic wall temperature, T_{aw}, is typically 1.03). For the tested freestream Mach number of 4.0, the characteristics of the undisturbed boundary-layer at a position 22.7 cm downstream of the flat plate leading edge (which is close to the location of fin leading edge) is given as $\delta \cong 3.1$ mm, $\delta^* \cong 1.0$ mm, $\theta \cong 0.12$ mm, and $Re/l \cong 7.6E6/m$, where Re/l is the Reynolds number per unit length.

2.5 Instrumentation and data acquisition

The RTDs measure the temperature by change of the resistance of the sensing element according to a prior calibration. The constant current mode in the anemometer (TSI model 1050) is selected for this purpose. The frequency response of the present setup through the anemometer is tested by square-wave test and results in the range of more-than 40 kHz.

A LeCroy waveform recorder controlled by IBM microcomputer is used for data acquisition. It has 12 channels of high-speed data sampling capability at rates up to 5 MHz and 32 channels of relatively low-speed data sampling at rates up to 5 kHz. All these channels utilize 12-bit digitization. The "ASYST" software package is employed for data handling. 128K data points at 100 kHz sampling rate per sensor per tunnel run are taken for the data acquisition. This sample size is large enough to ensure the convergence of the calculation of its statistics. The unimportant signal from each sensors is rejected by using the low-pass precision filter (model 6602B) in cutoff frequency of 45 kHz, and amplified prior to digitization.

3. Results and Discussion

Various fin angles with different freestream Mach numbers can generate different interaction strengths from weak to very strong. In the present experiment two different interactions ($M_\infty = 4.0$, fin angles $\alpha = 16°$, 20°) are chosen for test.

3.1 Characteristics of incoming boundary-layer

A simple test to access the magnitude of electric room noise, keeping the instrumentation settings the same as for the wind-tunnel tests is carried out. The rms (standard deviation) noise level is then compared with its level measured beneath the undisturbed incoming boundary-layer on the flat plate (at the location of 24.9° with respect to the fin leading-edge) without swept shock, as shown in Fig. 3(a).

From this figure, the rms electric noise level is found to be approximately one-sixth of the rms level of flat plate boundary-layer of Mach 4.0. Although only the signal from one RTD is compared in the figure, the trends of the room-noise and flat plate boundary-layer signals from other RTDs are found to be almost identical. Fig.

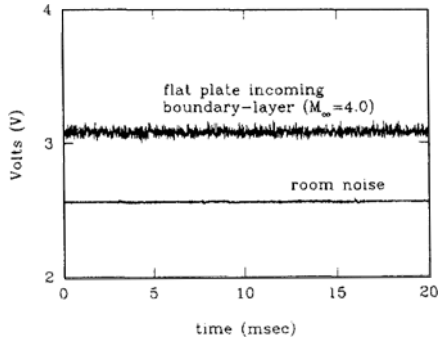

(a) comparison with room nosie

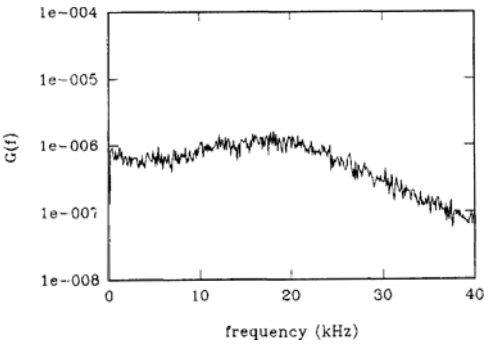

(b) power spectrum

Fig. 3 Signals of flat plate boundary-layer.

3(b) shows the result of power spectra calculation (1024-point fast Fourier transforms are averaged giving a frequency resolution of 97.7 *Hz*) carried out using only AC components of the same signal. As expected, the spectra are broadband, which is a typical characteristics of the turbulent boundary-layer on a flat plate. The probability density distribution is also calculated for the same signal, and found to be Gaussian.

3.2 Interaction measurements

Distribution of raw values : The surface temperature fluctuation levels for the interaction of M_∞= 4.0, α=16° are compared along the angle β in Fig. 4.

As shown in the figure, the fluctuation levels underneath the λ-shock structure (25.6°$\leq\beta\leq$38.9°) are stronger compared to its level of the undisturbed boundary-layer (β=47.1°). High frequency component of the fluctuation near the reattachment of the separated incoming boundary-layer (β=24.0°) is also observed. At this location of reattachment, the highest level of heat transfer (steady-state) has been observed by Lee et al.

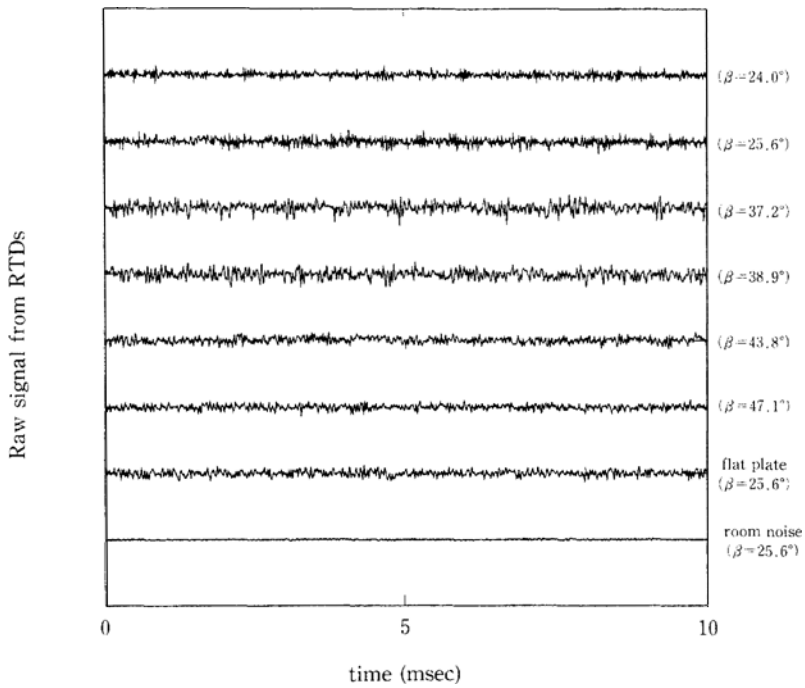

Fig. 4 Time-history plot of surface temperature fluctuation (M_∞=4.0, α=16°).

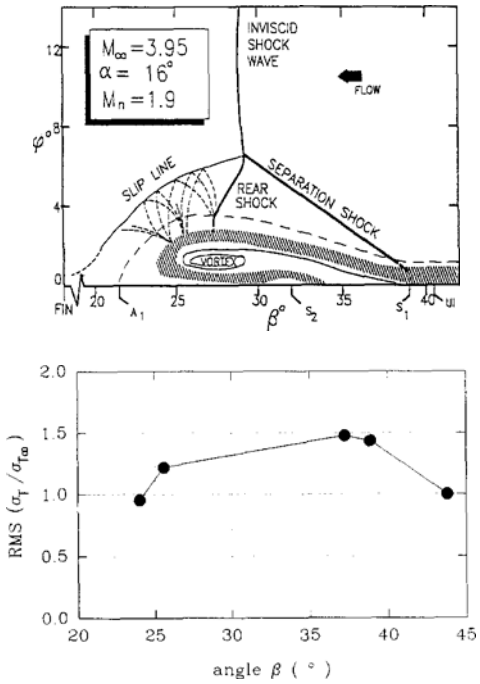

Fig. 5 Flowfield map and rms temperature fluctuation for $M_\infty=4.0$, $\alpha=16°$.

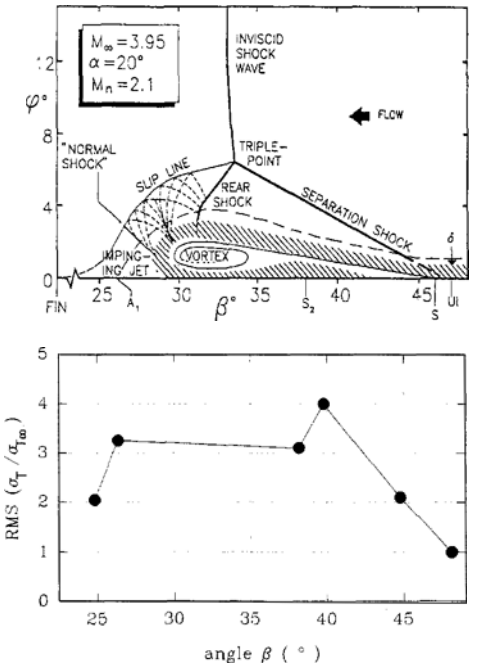

Fig. 6 Flowfield map and rms temperature fluctuation for $M_\infty=4.0$, $\alpha=20°$.

(1994). In the previous studies of surface pressure fluctuations in the similar type of interactions (Dolling and Murphy, 1983 ; Garg and Settles, 1996), low-frequency, intermittent characteristics of the fluctuations have been observed near the primary separation ($\beta\sim40°$ for the present case, see Fig. 5). They postulated that those features were due to the oscillating motion of the separation shock. Unfortunately, RTD near $\beta=40°$ in the present test is broken by an accidental high current through it and no data has been obtained to check the similar type of fluctuations of temperature.

RMS distributions : Distributions of rms temperature fluctuation level, σ_T, for the two different interactions are shown in Figs. 5 and 6. The present rms level is normalized by its level of the undisturbed incoming boundary-layer of mach 4, $\sigma_{T\infty}$. The flowfield maps proposed by Alvi and Settles (1991) for these two interaction cases are also shown in the top of the figures for a comparsion. In the flowfield map, the surface flow features are indicated. Here, S_1, S_2, A_1, and UI represent the primary separation, secondary, separation, primary reattachment and upstream influence, respectively. These angles of the surface limiting streamlines are measured by a surface flow visualization technique (kerosene-lampblack tracing) within the accuracy of 2°.

In Fig. 5 ($M_\infty=4.0$, $\alpha=16°$), the rms level begins to rise after the upstream influence line and it is maximized near the secondary separation and drops near the primary reattachment where the jet of separated flow impinges. Although Garg and Settles (1996) have observed a strong jump in the fluctuation of surface pressure level near the primary separation and irregular up-and-down variation of it near the reattachment ($M_\infty=3.0$, $\alpha=20°$), similar characteristic of temperature flucturations is not observed for the present experiment, partly due to the several broken sensors. Even though Shifen and Qingquan (1990) have observed that the weaker heat transfer fluctuation level near the reattachment than near the primary separation, the drop of temperature fluctuation ratio to 1.0 near the reattachment in Fig. 5 is not fully understood at the present time. In Fig. 6 ($M_\infty=4.0$, $\alpha=20°$) which represents the stronger

interaction, a sharp increase of the rms level from the primary separation to the secondary separation can be seen and its maximum rms level also gets larger.

To compare again the present results with Garg and Settles' (1996) observation, the probability density distribution is calculated for $\beta=44.8°$ which close to the primary separation for $M_\infty=4.0$, $\alpha=20°$. The result is shown in Fig. 7. Here, P (T), μ_T and T represent the probability density function, mean value and temperature, respectively. Its distribution is similar to the normal distribution shown in solid line in the figure, and gives no hint of intermittence.

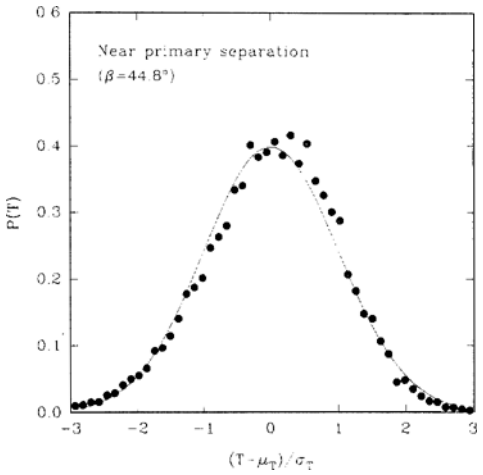

Fig. 7 Probability density distribution at $\beta=44.8°$ for $M_\infty=4.0$, $\alpha=20°$.

Power spectra of fluctuations Figures 8 and 9 show the power spectra from the present $M_\infty=4.0$, $\alpha=16°$ and $\alpha=20°$ interactions for various locations of β. Only AC component of the fluctuation signal is utilized to calculate the power spectra, and the frequency up to 40 *kHz* is shown in the figures. As expected, the incoming boundary-layer spectra outside the upstream influence line ($\beta=41°$ for $\alpha=16°$, and $\beta\cong48°$ for $\alpha=20°$, see Figs. 5 and 6) are broadband and flatten up, which is the typical characteristics of the turbulent boundary-layer. However, after primary separation, a slight increase in energy at higher frequencies is observed. This phenomenon is identical to the previous results of surface pressure fluctuation at the same type of the interaction (Garg and Settles, 1996). However, an interesting result is observed near the reattachment of the separated flows. Further downstream, under the

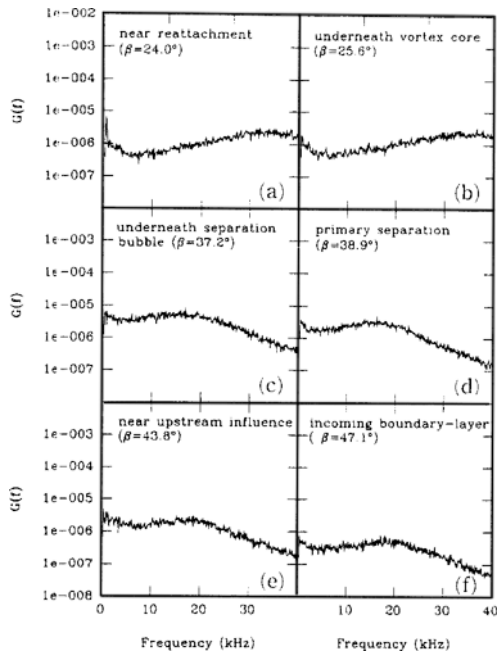

Fig. 8 Power spectra of wall temperature fluctuations for the interaction of $M_\infty=4.0$, $\alpha=16°$.

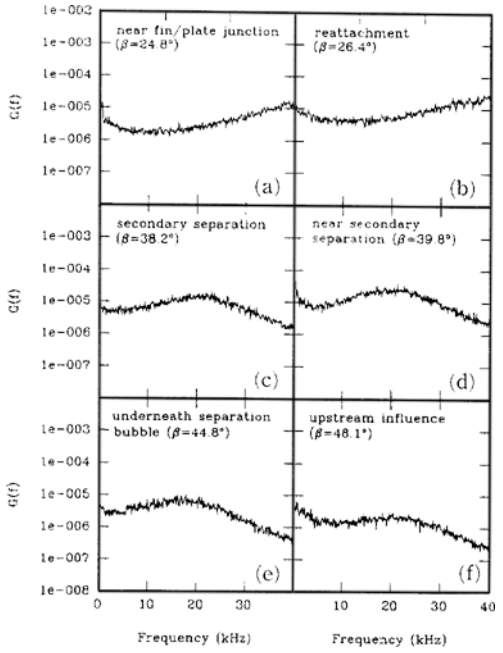

Fig. 9 Power spectra of wall temperature fluctuations for the interaction of $M_\infty=4.0$, $\alpha=20°$.

separation bubble (near the reattachment), the increased energy is focused on the higher frequency range of 20~40 *kHz* (Figs. 8(a) and 8 (b), 9(a) and 9(b)). According to Garg and Settles' (1996) power spectra obtained from surface pressure fluctuations, an increase in energy is dominated by relatively low frequencies in the range of 0~5 *kHz* near reattachment. They postulated that this might be due to the flapping motion of the primary separation line (also see Gramann Dolling, 1990). By an experimental study of fluctuation of heat transfer in two -dimensional shock/boundary-layer interactions, Hayashi et al. (1988) have shown that the fluctuation of heat transfer are strong near the separation and reattachment points. However, their measurements were restricted to only its magnitude not spectra due to the relatively slow response (600 *Hz*) of their sensors. Although the contrary between the fluctuation pressure load and thermal load near reattachment in the interaction is not clearly explained, the following consideration on the feature is possible : while the surface pressure fluctuations in the interaction are intimately related to the behavior of the flowfield off the surface, especially to the low-frequency flapping motions of the primary separation, the fluctuation of thermal loads near the reattachment in the interactions is more sensitive to the small scale turbulent structures near the wall. More extensive experimental studies on the detailed mechanism of small scale turbulence structures, such as two -point measurements, are still needed to derive more definite conclusion.

4. Conclusions

An experimental research program establishing data on the fluctuation of thermal loads in swept shock/boundary-layer interactions is described. For each of two different strong interaction cases of freestream Mach number 4.0, surface temperature fluctuations are read from two streamwise rows of 37 RTDs connected to anemometer. Major conclusions from the present experimental study can be summarized as follows :

(1) The rms level of surface temperature fluctuations underneath the λ-shock structure is higher than its level of the incoming boundary-layer, and its magnitude becomes larger as the interaction strength get stronger.

(2) The fluctuation of thermal loads near the reattachment of the separated boundary-layer in the interaction has high-frequency components which are not negligible.

References

Alvi, F. S., Settles, G. S., 1991, "Physical Flowfield Model of the Swept Shock/Boundary-Layer Interaction Flowfield," *AIAA Paper* 91-1768.

Dolling, D. S. and Murphy, M T., 1983, "Unsteadiness of the Separation Shock Wave Structure in a Supersonic Compression Ramp Flowfield," *AIAA Journal*, Vol. 21, No. 12, pp. 1628~1634.

Dolling, D. S., 1993, "Fluctuating Loads in Shock Wave/Turbulent Boundary-Layer Interactions : Tutorial and Update," *AIAA* paper 93-0284.

Erengil, B. and Dolling, D. S., 1993, "Effects of Sweepback on Unsteady Separation in Mach 5 Compression Ramp Interactions," *AIAA Journal*, Vol. 31, No. 2, pp. 302~311.

Garg, S. and Settle, G. S., 1996, "Unsteady Pressure Loads Generated by Swept-Shock-Wave/Boundary-Layer Interactions," *AIAA Journal*, Vol. 34, No. 6, pp. 1174~1181.

Gibson, B., Dolling, D. S., 1991, "Wall Pressure Flucuations near Separation in a Mach 5, Sharp Fin-Induced Turbulent Interaction" *AIAA* Paper 91-0646.

Gramann, R. A. and Dolling, D. S., 1990, "Dynamics of the Outgoing Turbulent Boundary Layer in a Mach 5 Compression Ramp Flow," *AIAA* paper 90-1645.

Hayashi, M., Aso, S. and Tan, A., 1988, "Fluctuation of Heat Transfer in Shock Wave/Turbulent Boundary-Layer Interaction," *AIAA* Paper 88-0426.

Kim, K-S., Lee, Y., Alvi, F. S., Settles, G. S., Horstman, C. C., 1991, "Laser Skin Friction Measurements and CFD Comparison of Weak-to-

Strong Swept Shock/Boundary Layer Interactions," *AIAA Journal*, Vol. 29, No. 10, pp. 1643 ~1650.

Kistler, A. L., 1964, "Fluctuating Wall Pressure Under a Separated Supersonic Flow," *Journal of the Acoustical Society of America*, Vol. 36, March, pp. 543~550.

Lee, Y., Settles, G. S., Horstmann, C. C., 1994, "Heat Transfer measurements and Computations of Swept-Shock-Wave/Boundary-Layer Interactions," *AIAA Journal*, Vol. 32, No. 4, pp. 726 ~734.

Lu, F. K., Settles, G. S., 1983, "Conical Similarity of Shock/Boundary-Layer Interactions Generated by Swept Fins," *AIAA* Paper 83-1756.

Lu, F. K., 1988, "Fin Generated Shock-Wave Boundary-Layer Interactions," Ph. D. thesis, ME dept., The Pennsylvania State University.

Settles, G. S., Dolling, D. S., 1986, "Swept Shock Wave Boundary-Layer Interactions," in *AIAA Progress in Astronautics and Aeronautics* : Tactical missile Aerodynamics, edited by M. Hemsch and J. Nielsen, Vol. 104, pp. 297 ~379, AIAA, New York.

Settles, G. S., Dolling, D. S., 1990, "Swept Shock/Boundary-Layer Interactions-Tutorial and Update," *AIAA* paper 90-0375.

Shifen, W. and Qingquan, L., 1990, "Nature of the Surface Heat Transfer Fluctuation in a Hypersonic Separated Turbulent Flow," *ACTA MECHANICA*, Vol. 6, No. 4.

Zubin, M. A. and Ostapenko, N. A., 1979, "Structure of Flow in the Separation region Resulting from Interaction of a Normal Shock Wave with a Boundary Layer in a Corner," Izvest. Akad. Nauk S.S.S.R., Mekh. Zhid. i Gaza, No. 3, 51-58, (English translation).